

Lessons on textile history and fibre durability
from a 4000-year-old Egyptian flax yarn

Authors: Alessia Melelli¹, Darshil U. Shah², Gemala Hapsari³, Roberta Cortopassi⁴, Sylvie Durand⁵, Olivier Arnould⁶, Vincent Placet³, Dominique Benazeth⁴, Johnny Beaugrand⁵, Frédéric Jamme⁷, Alain Bourmaud^{1,*}.

¹ Univ. Bretagne Sud, UMR CNRS 6027, IRDL, Lorient, France.

²Centre for Natural Material Innovation, Department of Architecture, University of Cambridge, Cambridge CB2 1PX, United Kingdom

³FEMTO-ST Institute, Department of Applied Mechanics, UMR CNRS 6174, University of Franche-Comté, 25000 Besançon, France

⁴Musée du Louvre, Département des Antiquités Egyptiennes, 75058 Paris cedex 1, France.

⁵INRAE, UR1268 BIA Biopolymères Interactions Assemblages, 44316 Nantes, France

⁶LMGC, Université de Montpellier, UMR CNRS 5508, Montpellier, France

⁷Synchrotron SOLEIL, DISCO beamline, Gif-sur-Yvette, France

*Correspondence to: alain.bourmaud@univ-ubs.fr

Flax has a long and fascinating history. This plant was domesticated around 8,000 BCE¹, in the Fertile Crescent area², first for its seeds and then for its fibres^{1,3}. Although, its uses existed long before domestication - residues of flax yarn dated 30,000 years ago have been found in the Caucasus area⁴. However, it is Ancient Egypt which laid the foundations for the cultivation of flax as a textile fibre crop⁵. Today, flax fibres are used in high-value textiles, as well as natural actuators⁶ or reinforcements in composite materials⁷. Flax is therefore a bridge between ages and civilizations. For several decades, the development of non- or micro-destructive analysis techniques has led to numerous works on the conservation of ancient textiles. **Non-destructive methods such as optical microscopy⁸, or vibrational techniques^{9,10} have been largely used to investigate archaeological textiles, principally to evaluate their degradation mechanisms and state of conservation. Vibrational spectroscopy studies can now benefit from synchrotron radiation¹¹ as well X-ray diffraction (XRD) measurement in the archaeometric study of historical textiles^{12,13}.** Conservation of mechanical performance and the ultrastructural differences between ancient and modern flax varieties have not been examined thus far. **Here, in order to assess the quality and durability of ancient flax fibres and relate this to their processing methods,** we examine the morphological, ultrastructural and mechanical characteristics of a yarn from an Egyptian mortuary linen, dating from the early Middle Kingdom (Eleventh dynasty, ca. 2033 - 1663 BCE), and compare them against a modern flax yarn. **Advanced microscopy techniques, such as nano-tomography, multiphoton excitation microscopy and atomic force microscopy were used.** Our findings reveal the cultural know-how of this ancient civilization in producing high-fineness fibres, as well as the exceptional durability of flax, which is sometimes questioned, demonstrating their potential as reinforcements in high-tech composites.

The most beautiful fabric pieces of flax date from Ancient Egypt (Fig. 1), their highly-preserved state a result of their optimal conservation over millennia in coffins or tombs with remarkably stable moisture and thermal conditions, as well as sheltering from UV light. Flax textiles were particularly prized by the Egyptians because of its comfort and the fineness of its fibres¹⁴. Flax was widely used for clothing (Fig 1.a) and in the fishing sector for work clothes, felucca sails and nets. The funerary uses included mummy strips (Fig 1.b), funeral linen (Fig 1.c, d, g) as well as ornaments (Fig 1.e).

In terms of cultivation, the fertile Nile valley with its light and rich or sandy soils was particularly suitable for flax. After growing, the stems were pulled out, as shown in illustrations found in the tomb of Sennedjem (Deir el Medineh, Egypt) and then probably water-retted. Over the past century or so, growth conditions have changed and varietal selection has significantly increased the crop's fibre yields¹⁵. It is therefore difficult to compare varieties across the ages. Even so, an in-depth study of 407 flax genotypes of different origins has shown that regions that have been the centre of origin of the crop, such as the Mediterranean or Abyssinia, highlight haplotypes that are more unique than the temperate group and are representative of oil-seed plants¹⁶.

According to Braun¹⁷, the flax found in the lake dwelling does not belong to the species now cultivated (*Linum usitatissimum* L) but to the *Linum angustifolium* which is not cultivated at the present time. Today's cultivated flax *Linum usitatissimum* L. is considered as being domesticated from the wild progenitor pale flax *Linum angustifolium* Huds. Both have phenotypic characters of great heritability, and are distinguishable by several characteristics, such as the length and width of petals, size of seeds, colour and shape of the flower, height of plants but also the number of days until emergence from the soil or flowering¹⁸. However, the height of the plants shown on the Egyptian bas-reliefs¹⁹ as well as the size of the seeds found during excavation¹ suggests that the species cultivated by the Egyptians were morphologically close to those we know today.

Figures 2.a and 2.d compare the overall architecture, observed by SEM, of old (Fig. 1.g and Supplementary Fig.1.a) and modern (Supplementary Fig.1.b) flax yarn, respectively. Despite a lower level of twist (about 180 turns per metre (tpm) against 320 tpm for the modern flax), the old flax possesses a similar metric number (about 122 tex or 8.2 km/kg), showing the mastery of the Egyptians in manual spinning. Figure 2.b reveals the level of individualisation of the fibres. In the flax stem, fibres are aggregated in cohesive bundles made of several tens of fibres, the latter being more or less divided after retting and extraction stages. The old yarn is mainly made up of elementary flax fibres; the residues of cortical parenchyma and middle lamellae are very few. This demonstrates the effectiveness of the water-retting process utilized at the time as Pliny the Elder explained²⁰. Water-retting enables homogeneous retting and, when it is well executed, enables the production of very fine fibres. One can notice that the low fibre yield in ancient flax varieties can also lead to easier retting and fibre division²¹. In modern flax fibre extraction processes, stems undergo field retting over several weeks. Dependent on natural weather conditions, this can lead to retting heterogeneity. As a consequence, numerous residues of pectic intermediate lamellae or cortical parenchyma are visible on the modern flax yarn (Fig. 2.e, h). Such residues increase roughness of the yarn and are detrimental to the sensation of comfort (e.g. softness). This is in contrast to the reputation of Egyptian flax fabrics, whose most beautiful specimens were reserved for members of high society. These observations validate the important know-how of ancient Egyptians in textile manufacturing. The scanning electron micrographs (Figs. 2.a, b) also reveal the excellent general conservation of the ancient fibrous yarns.

Figures 2.g and 2.h present cross-sections of the old and modern yarn observed in nano-tomography and Figure 2.i illustrates the analysed distribution in elementary fibre diameters for the two materials. The mean diameters are $14.3 \pm 3.3 \mu\text{m}$ for the fibres in the old yarn ($n = 523$) and $17.6 \pm 3.6 \mu\text{m}$ for the modern yarn ($n = 208$); both diameter values are consistent with

typically reported values on flax fibres²². A significant difference in elementary fibre diameters is observed and confirmed by a student test with $P \leq 0.001$. The smaller diameters of old flax may be related to the plant variety, the weather conditions during growth (hydric stress, for example)²³, and/or even the sampling area within the stem, with larger diameter fibres being generally located in the middle section of the stem height²⁴. The retting method utilized may also explain the differences and scatter in elementary fibre diameters between the old and modern flax yarn (Fig. 2.i). The use of water-retting for the old flax yarn, leads to completely separated fibres and free from surface residues (Fig. 2.b). This further demonstrates the skill of the ancient Egyptians in obtaining fine yarns and textiles.

Differences are also visible in the size of the lumens, with SEM and tomographic images (Fig. 2.c, f, g and h) showing larger ones for old flax fibres. While the lumens of modern flax fibres represent only a few percent of the total surface area²⁵, here, old fibres possess lumens of the order of 30-40%, comparable to wood or coconut fibres²⁵. We hypothesize that these low wall thicknesses of old flax may be due to a premature halt in the cellulose filling process of the cell walls following the intrusive growth phase²⁴. This filling can be interrupted by extreme weather conditions, such as lodging or marked periods of hydric stress²⁶.

Flax fibres are characterised by their multi-layered structure and their generally polygonal shape, as well as by the presence of structural defects known as kink-bands²⁷, distributed along the fibre length. Notably, the relative quantity and size of these kink-bands is particularly large on old fibres (Fig. 2.b, Fig. 3.a, b) in comparison to modern fibres (Fig. 3.d, e). The origin of these defects is not well known but the plant fibre community generally attributes them to mechanical stresses induced during the extraction or processing of the stems, but also to residual stresses that may be released during periods of stem or fibre drying, possibly during the retting stage^{27,28}. The large quantity of kink-bands on old flax fibres may be the result of aggressive decortication, scutching or spinning processes used by the Egyptians following

water-retting, but may also be caused by progressive release of internal stresses over the 4 millennia. In flax fibres, kink-bands modify the aesthetics and regularity of the fibres, and are also considered as zones of weakness, especially when utilized in a fibre-reinforced composite²⁹. Kink-bands also make the fibre more susceptible and sensitive to ageing by acting as entry points for microorganisms or moisture to access the inner layers of the cell walls³⁰.

We specifically examined the kink-bands through multiphoton microscopy with second harmonic generation imaging, which highlights crystalline cellulose within the plant cell walls. Figure 3.c shows discontinuity and disorganization of crystalline cellulose in the kink-band of old flax, and possibly indicate areas of low crystallinity in this region. Both these factors would cause kink-band rich ancient flax fibres to be more brittle¹³. Indeed, these old fibres have proved to be very fragile during handling, and impossible to isolate without breaking/damaging them for any single-fibre tensile testing.

Finally, atomic force microscopy tests in peak force quantitative nano-mechanical (AFM-PF-QNM) mode were conducted on transverse cross sections of old and modern flax fibres. Such measurements (Fig. 4) allow estimation of the indentation modulus of flax plant cell walls, i.e., do not depend on the relative lumen size and are a useful measure for highlighting mechanical property gradients or heterogeneities within cell walls³¹. Interestingly, we found that the AFM mechanical properties are slightly higher for cell walls of old flax than those of modern flax, i.e., 23.7 ± 0.2 GPa and 20.3 ± 0.1 GPa, respectively; for each batch, 2,500 indentation moduli values were statistically compared and the student t-test confirmed that the two sets of moduli are different with $P \leq 0.001$. Values of modern flax are in line with the measurements in the literature²⁵ and measured by nanoindentation (Supplementary Tab.1). Measurements by infrared spectroscopy (Supplementary Fig. 6 and Supplementary Tab.2) revealed a lower intensity of peaks attributed to parietal hemicelluloses for old flax. It has been shown that the longitudinal and transverse shear moduli of the fibres³² and especially the stiffness of the non-

cellulosic matrix of the plant cell walls³³ have a major effect on the indentation modulus; our results confirm this important influence of hemicelluloses, even though they are the softest component of the cell wall, on the indentation modulus. Higher indentation modulus has previously been recorded on old wood samples and is attributed to a loss of pectins, as well as modification of the ligno-cellulosic cell wall polymers³⁴. The wider literature supports the hypothesis of a significant evolution in the ageing sensitive hemicellulosic polymers over 4,000 years. Differences in crystallinity were also checked through both nuclear magnetic resonance (NMR) and X-Ray diffraction (XRD) measurements; Supplementary Figure 7 shows that the cellulose crystallinity measured by both NMR (58.0% for Egyptian yarn and 56.0% for the modern yarn) and XRD (59.6% for Egyptian yarn and 58.4% for the modern yarn) techniques is comparable between the ancient and modern flax yarns. Moreover, the measured indentation moduli are homogeneous in the fibre sections and show little dispersion, suggesting no ageing gradient across a fibre transverse section. Such quantitative nano-structural measurements, never before conducted on such ancient fibres, reveal the durability of these flax plant cell walls. Even though at the fibre-scale, the kink-bands are regions of pronounced damage, the cell walls themselves exhibit a moderate change in their elastic performance despite their age; only a slight increase in their stiffness, connected to the evolution of their non-cellulosic polysaccharide composition, is demonstrated.

Our structural examination of 4000-year old Egyptian flax fibres in comparison to modern flax fibres has offered a number of insights on the textile know-how of the Egyptians, as well as on the temporal evolution of flax fibres. Through water retting and manual processing, the ancient Egyptians could separate the flax into very fine fibre bundles and in most cases even into single fibres to make soft and luxurious quality textiles despite fully-manual processing. Local nanomechanical measurements show an increase in cell wall stiffness of old fibres, probably induced by the alteration of non-cellulosic polymers, as cellulose retained a crystallinity close to

that of contemporary fibres. In addition, a larger presence of structural defects – stress-concentrating kink-bands with low cellulose crystallinity – is notable on the old, fragile fibres. In future and in work-in-progress, we aim to go further by exploring the microfibrils angle (MFA) values of ancient flax (through single fibre XRD and SHG), the internal structure of kink-bands (by nanotomography) and if possible, to gain information on the Linum used by ancient Egyptians thanks to genetic analysis. To improve durability at the fibre scale, producing fibres with low quantities of defects is necessary, in particular if they are to be used as reinforcements of next-generation environmentally-friendly composite materials. Intriguingly, the ancient Egyptians had also dabbled their hands in making the first linen/plaster cartonnage biocomposites for death masks, a number of which survive to date (Fig. 1.b).

Methods

Materials

Two samples of flax yarns were studied (Supplementary Fig. 1), an ancient and a contemporary sample, referred to as old and modern flax, respectively, in the manuscript. The large linen tabby, bordered with a fringe (inv. E 13595, Supplementary Fig. 1.a) was given in 1929 by Georges Daressy, former General Secretary of the Antiquity Service in Egypt, to the Louvre Museum (Paris, France). Its provenance is unknown but this piece of shroud most likely came from a tomb, because all the textiles of ancient Egypt were found in cemeteries. These cemeteries were located in the desert in order to ensure dryness and optimal conservation of the burials. Indeed, in the valley, the annual flooding of the Nile was too risky. Thus, the Egyptian climate of the desert areas, which was exceptionally dry and favourable to the proper conservation of organic materials, made it possible to find many fabrics in excellent condition. The linen was radiocarbon dated in 2009 (Laboratoire de Mesure du Carbone 14, CEA-Saclay,

Gif-sur-Yvette Cedex, France): it had been harvested between 2140 and 1976 BC (with 95.4% probability), during the 9th, 10th or 11th dynasties, a period known as the First Intermediate Period and the beginning of the Middle Egyptian Kingdom. Morphological characteristics of the ancient yarn were calculated from **mass** measurements and from image analysis. The **linear density** and twist of this old yarn are **122 tex** and **180 tpm**, respectively. In addition, a contemporary yarn was used (Supplementary Fig. 1.b). It was produced from textile flax (Melina variety) cultivated in 2018 in Normandy (France) by Teillage Saint-Martin company; this flax was dew-retted conventionally over 6 weeks and then scutched and hackled (Bourmaud et al. 2018 PMS). Then, it was wet spun by Safilin Pionki (Poland) with a **linear density** and twist of **105 tex** and **320 tpm**, respectively.

SEM observations

For each of the two yarns, a sample of a few millimetres was used. A Jeol JSM 6460LV scanning electron microscope was used to analyse the flax yarns; **secondary emission electrons were used, and the accelerating voltage was 3.0 kV**. They were glued to a sample holder using a conductive adhesive and then metallized with a thin layer of gold using an Edwards Scancoat Six device for 180 s.

Multiphoton microscopy

Preparation of samples

An elementary fibre was extracted from the modern flax yarn and mounted on paper support commonly used for tensile tests according to ASTM C1557 and fixed with universal glue. The sample prepared was placed between two coverslips and scanned. In contrast, the preservation state of the Egyptian yarn does not allow to extract elementary fibres, which are more brittle, so a whole **collective** of less than 1 cm was mounted on paper support commonly used for tensile tests but glued in the horizontal direction in order to use the aperture of 5 mm.

The sample prepared was placed between two coverslips and scanned by the multiphoton microscope. The samples were mounted at 90° to the initial laser polarization position.

Second harmonic generation (SHG) microscopy imaging

SHG imaging was performed with a multiphoton Nikon A1 MP+ microscope (NIKON, France) equipped with a long working distance (LWD) 16x (NA 0.80) water immersion objective (NIKON, France). The system is equipped with a tuneable Mai Tai XF mode-locked Ti:sapphire femtosecond laser (SPECTRA PHYSICS, France) and a half-wave plate (MKS-Newport, USA) in front of the laser excitation beam. The half-wave plate was rotated to change the laser polarisation angle until to reach the maximum intensity SHG signal of both flax yarns (maximum signal reached 2°-3°). The excitation wavelength chosen was 810 nm (average power at 1.5 W) to obtain the maximum of the performance from the filters equipped (SH collected with a bandpass filter at 406/15 nm), and the maximum laser power percentage used was 2% for the Egypt yarn and 5% for the modern yarn to avoid the bleaching of the surface. We collected both autofluorescence and SHG signals by GaAsP NDD (gallium arsenide non-descanned) detectors. The scan line average was 16, the scan velocity was fixed at 1 (fps) and the scan size was 512x512pixels. All the measurements were performed at room temperature and dry ambient.

X-ray tomography measurements

The yarns' microstructure was characterized using X-ray nanotomography. Image acquisition was realized on an EasyTom RX Solutions micro/nano tomograph (RX Solutions, Chavanod, France). A Lanthanum hexaboride (LaB6) filament was used as cathode with a voltage of 50 keV and a current of 100 µA, leading to a resolution of 0.5 µm. The anode was in beryllium and has a thickness of 0.5 mm. Resolution of the micro-CT images was set to 4.44 µm/pixel. The imager used was a Fluoroscopic High Speed imaging sub-system PaxScan

2520DX and the scintillator was produced with a direct deposition of Cesium Iodide (CsI). To obtain optimum measurement contrast, the framerate has been set to 0.25 fps. In addition, in order to minimize the measurement noise, each projection obtained was the result of the averaging of 15 acquisitions. Finally, in order to obtain the most faithful reconstruction possible, the flax fibers were measured in 1440 different positions (angles). The yarn centering was carried out using a perforated carbon tube. The tube outside diameter was 1 mm and the inside hole diameter was 0.5 mm. A little bit of glue was used to maintain the yarns. The measured volume was 0.5 mm in diameter over a height of 0.8 mm with a resolution of 500 nm. In order to allow maximum beam stability from the start of the measurement, the wire was preheated 3 hours before the start of the measurement. In total, each measurement therefore lasted approximately 27 hours. An X-ray radiograph is given in Supplementary Fig. 2.a to illustrate the measurement (the yarn is hardly perceptible). The reconstruction was carried out using Xact software using the filtered back-projection method. For the noise filtering, the apodization was done using a sine window with a threshold of 75% for the low pass filter. For the border filter a Tukey window type was used with a non-filtered area of 46%. For more information on filters and the effects of reconstruction filter on CBCT image quality see³⁵. Once the reconstruction has been carried out, the result is stored in the form of a slices stack. An illustration is given in Supplementary Fig. 2.b. Finally, the analyses and reconstruction of surfaces were carried out using the VGSTUDIO MAX software as illustrated on Supplementary Figs. 3.a and 3.b at two different scales.

Nano-mechanical investigations

Preparation of samples

A subsample of less than 1 cm was cut from the ancient flax yarn (Louvre) and modern flax yarn samples. The two subsamples were put in an oven at 60°C for two hours and then embedded in Agar resin (epoxy resin Agar Low Viscosity Resin (LV) -Agar scientific UK). The

blocks prepared were put back in the oven at 60°C overnight for the final polymerisation of the resin, then machined, to reduce their cross-section, and glued on a 12 mm AFM stainless steel mounting disk. The sample surface was thus cut using an ultramicrotome (Ultracut S, Leica Microsystems SAS, France) equipped with diamond knives (Histo and Ultra AFM, Diatome, Switzerland) to obtain thin sections (about 50 nm thick in the last step) at reduced cutting speed (~1 mm/s) to minimize compression and sample deformation during the cutting process, and thus reduce the sample surface damage and topography (Supplementary Fig. 4).

AFM PF-QNM investigations

A Multimode 8 Atomic Force Microscope (Bruker, Billerica, Massachusetts, USA) was equipped with a RTESPA-525 probe (Bruker probes, Billerica, Massachusetts USA) with a nominal spring constant of 200 N/m and a resonance frequency of 525 kHz. The actual spring constant was calculated with the Sader Method (<https://sadermethod.org/>). The AFM set-up was calibrated with the relative method using sapphire as hard standard material to calculate the deflection sensitivity and the PF-QNM synchronisation distance. A sample of aramid fibres K305 Kevlar Taffetas 305 g/m² (Sicomine epoxy systems-France) accurately prepared in blocks of Agar resin (Agar Low Viscosity Resin (LV)-Agar scientific, UK), whose surface was prepared with the same protocol as the flax samples, was previously tested by nanoindentation and then used to calibrate the tip radius (aramid fibre ~24.3 GPa and embedded resin ~5.4 GPa). The range of the stiffness of the cantilevers used was between 109 and 161 N/m and the tip radius between 15 and 30 nm at the beginning of the measurements.

The fast scan axis angle was at 90°, the maximum of the peak force setpoint used was 200 nN, the oscillation frequency selected at 2 kHz, the Poisson's ratio used was set to 0 as the tested cell walls are anisotropic, thus the modulus measured is the indentation modulus. The maximum fast scan velocity was selected at 8 µm/sec and the image resolution set to 512x512 pixels. The gain was set in automatic mode.

Two to three different areas of each sample (old and modern respectively) were measured to obtain a better statistic but only one representative area for each sample is reported in this paper (Fig. 4, Supplementary Figs. 4 and 5). Supplementary Figure 4 shows the topography images corresponding to investigated areas of Figure 4. To obtain the indentation modulus values, the entire surface of the secondary S₂ (or G) wall of each fibre was selected; indentation modulus data were automatically calculated for each point from the force-distance curves with a DMT contact model using NanoScope Analysis software (Bruker, Billerica, Massachusetts, USA).

Consequently, for each sample, the indentation modulus calculated were obtained from two or three separate images and from between 80,000 and 140,000 points for each image analysed using Gwyddion free software (<http://gwyddion.net/>). Figure 9 shows the calculation mask, covering the investigated area for fibres of Figure 4. For each sample, histograms of Figure 4 represent the data obtained from all the images analysed; 206,613 and 364,575 AFM force curves were used for old and modern flax indentation modulus calculation, respectively.

Statistical analysis

A t-test was performed to quantify the statistical differences in fibre diameters and indentation moduli values between the old and modern fibres. P value was calculated for the two cases, with significance level $\alpha = 0.05$.

Acknowledgements

VP and GH sincerely thank Dr. Pierrick Malécot and the MIFHySTO research platform (FEMTO-ST, UTINAM and ICB institutes) at Université Bourgogne Franche-Comté (UBFC) for the technical and scientific support provided for nanotomography experiments; Xavier Falourd and Loïc Foucat (INRAE) are also thanked for NMR investigations. The authors want to thank the INTERREG IV Cross Channel programme for funding this work through the FLOWER project (Grant number n°23). SOLEIL Synchrotron is also thanked for funding the 99180266 and 99200015 in-house proposals. This work has also been supported by the EIPHI Graduate school (contract "ANR-17-EURE-0002").

Author contributions

A.B. and D.U.S designed this work. A.M., G.H., O.A., S.D., V.P., J.B., F.J. and A.B. collected and analyzed data. A.B., A.M. and D.U.S wrote and revised the paper with contributions from G.H., R.C., O.A., V.P., D.B., S.D., J.B. and F.J.

Competing interests statement

The authors declare no competing interests.

Data availability

The data that supports the plots within this paper and the findings of this work are available from the corresponding author on reasonable request.

Code availability

The open-source and commercial software used for data analysis are referenced in the Methods section.

References

1. Van Zeist, W. & Bakker-Heeres, J. A. H. Evidence for linseed cultivation before 6000 bc. *J. Archaeol. Sci.* **2**, 215–219 (1975).
2. Hopf, M. Plant remains and early farming in Jericho 1. in *The Domestication and Exploitation of Plants and Animals*. (ed. Dingleby, G.) (2008).
3. Herbig, C. & Maier, U. Flax for oil or fibre? Morphometric analysis of flax seeds and new aspects of flax cultivation in Late Neolithic wetland settlements in southwest Germany. *Veg. Hist. Archaeobot.* **20**, 527 (2011).
4. Kvavadze, E. *et al.* 30,000-Year-Old Wild Flax Fibers. *Science* (80-.). **325**, 1359 (2009).
5. Heer, O. Prehistoric culture of flax. *Nature* **453** (1873).
6. Le Duigou, A. & Castro, M. Evaluation of force generation mechanisms in natural, passive hydraulic actuators. *Sci. Rep.* **6**, 18105 (2016).
7. Mohanty, A. K., Vivekanandhan, S., Pin, J.-M. & Misra, M. Composites from renewable and sustainable resources: Challenges and innovations. *Science* (80-.). **362**, 536–542 (2018).
8. Bruni, S. *et al.* Analysis of an archaeological linen cloth: The shroud of Arquata. *Radiat. Phys. Chem.* **167**, 108248 (2020).
9. Edwards, H. G. M., Ellis, E., Farwell, D. W. & Janaway, R. C. Preliminary Study of the Application of Fourier Transform Raman Spectroscopy to the Analysis of Degraded

- Archaeological Linen Textiles. *J. Raman Spectrosc.* **27**, 663–669 (1996).
10. Kavkler, K., Gunde-Cimerman, N., Zalar, P. & Demšar, A. FTIR spectroscopy of biodegraded historical textiles. *Polym. Degrad. Stab.* **96**, 574–580 (2011).
11. Kavkler, K., Šmit, Ž., Jezeršek, D., Eichert, D. & Demšar, A. Investigation of biodeteriorated historical textiles by conventional and synchrotron radiation FTIR spectroscopy. *Polym. Degrad. Stab.* **96**, 1081–1086 (2011).
12. Müller, M. *et al.* Identification of ancient textile fibres from Khirbet Qumran caves using synchrotron radiation microbeam diffraction. *Spectrochim. Acta Part B At. Spectrosc.* **59**, 1669–1674 (2004).
13. Herrera, L. K. *et al.* Identification of cellulose fibres belonging to Spanish cultural heritage using synchrotron high resolution X-ray diffraction. *Appl. Phys. A* **99**, 391–398 (2010).
14. Weiss, E. & Zohary, D. The Neolithic Southwest Asian Founder Crops: Their Biology and Archaeobotany. *Curr. Anthropol.* **52**, S237–S254 (2011).
15. Botany of Flax. *Nature* **170**, 557–559 (1952).
16. Sertse, D., You, F. M., Ravichandran, S. & Cloutier, S. The genetic structure of flax illustrates environmental and anthropogenic selections that gave rise to its eco-geographical adaptation. *Mol. Phylogenet. Evol.* **137**, 22–32 (2019).
17. Braun, A. Plants of Ancient Egypt. *Sci. Am.* **173**, 2760 (1879).
18. Diederichsen, A. & Hammer, K. Variation of cultivated flax (*Linum usitatissimum* L. subsp. *usitatissimum*) and its wild progenitor pale flax (subsp. *angustifolium* (Huds.) Thell.). *Genet. Resour. Crop Evol.* **42**, 263–272 (1995).
19. Kawami, T. S. A Craft in Antiquity. *Science* (80-.). **256**, 1065–1066 (1992).
20. André, J. Nature du lin et horticulture. in *Plinie l’Ancien, Histoire naturelle* (ed. Budé) (1964).
21. Goudenhooff, C., Bourmaud, A. & Baley, C. Varietal selection of flax over time: Evolution of plant architecture related to influence on the mechanical properties of fibers. *Ind. Crops*

Prod. **97**, 56–64 (2017).

22. Baley, C. & Bourmaud, A. Average tensile properties of French elementary flax fibers. *Mater. Lett.* **122**, 159–161 (2014).

23. Chemikosova, S. B., Pavlencheva, N. V, Gur'yanov, O. P. & Gorshkova, T. A. The effect of soil drought on the phloem fiber development in long-fiber flax. *Russ J Plant Physiol* **53**, 656–662 (2006).

24. Bourmaud, A., Gibaud, M., Lefeuvre, A., Morvan, C. & Baley, C. Influence of the morphology characters of the stem on the lodging resistance of Marilyn flax. *Ind. Crops Prod.* **66**, 27–37 (2015).

25. Bourmaud, A., Beaugrand, J., Shah, D. ., Placet, V. & Baley, C. Towards the design of high-performance plant fibre composites. *Prog. Mater. Sci.* **97**, 347–408 (2018).

26. Goudenhooff, C., Bourmaud, A. & Baley, C. Study of plant gravitropic response: Exploring the influence of lodging and recovery on the mechanical performances of flax fibers. *Ind. Crops Prod.* **128**, 235–238 (2019).

27. Hernandez-Estrada, A., Gusovius, H.-J., Müssig, J. & Hughes, M. Assessing the susceptibility of hemp fibre to the formation of dislocations during processing. *Ind. Crops Prod.* **85**, 382–388 (2016).

28. Hughes, M. Defects in natural fibres: their origin, characteristics and implications for natural fibre-reinforced composites. *J. Mater. Sci.* **47**, 599–609 (2012).

29. Le Duc, A., Vergnes, B. & Budtova, T. Polypropylene/natural fibres composites: Analysis of fibre dimensions after compounding and observations of fibre rupture by rheo-optics. *Compos. Part A Appl. Sci. Manuf.* **42**, 1727–1737 (2011).

30. Foulk, J., Akin, D. & Dodd, R. Influence of pectinolytic enzymes on retting effectiveness and resultant fiber properties. *BioResources* **3**, 155–169 (2008).

31. Eder, M., Arnould, O., Dunlop, J. W. C., Hornatowska, J. & Salmen, L. Experimental micromechanical characterisation of wood cell walls. *Wood Sci. Technol.* (2012).

- 422 32. Jäger, A., Bader, T., Hofstetter, K. & Eberhardsteiner, J. The relation between indentation
423 modulus, microfibril angle, and elastic properties of wood cell walls. *Compos. Part A Appl.*
424 *Sci. Manuf.* **42**, 677–685 (2011).
- 425 33. Capron, M. *et al.* Mechanical characterization of developing tension wood fibre wall by
426 atomic force microscopy. in *8th Plant Biomechanics International Conference* 224–225.
427 (2015).
- 428 34. Bader, T. K., de Borst, K., Fackler, K., Ters, T. & Braovac, S. A nano to macroscale study
429 on structure-mechanics relationships of archaeological oak. *J. Cult. Herit.* **14**, 377–388
430 (2013).
- 431 35. Shaw, C. . *Cone Beam Computed Tomography*. (Taylor & Francis Group, 2014).

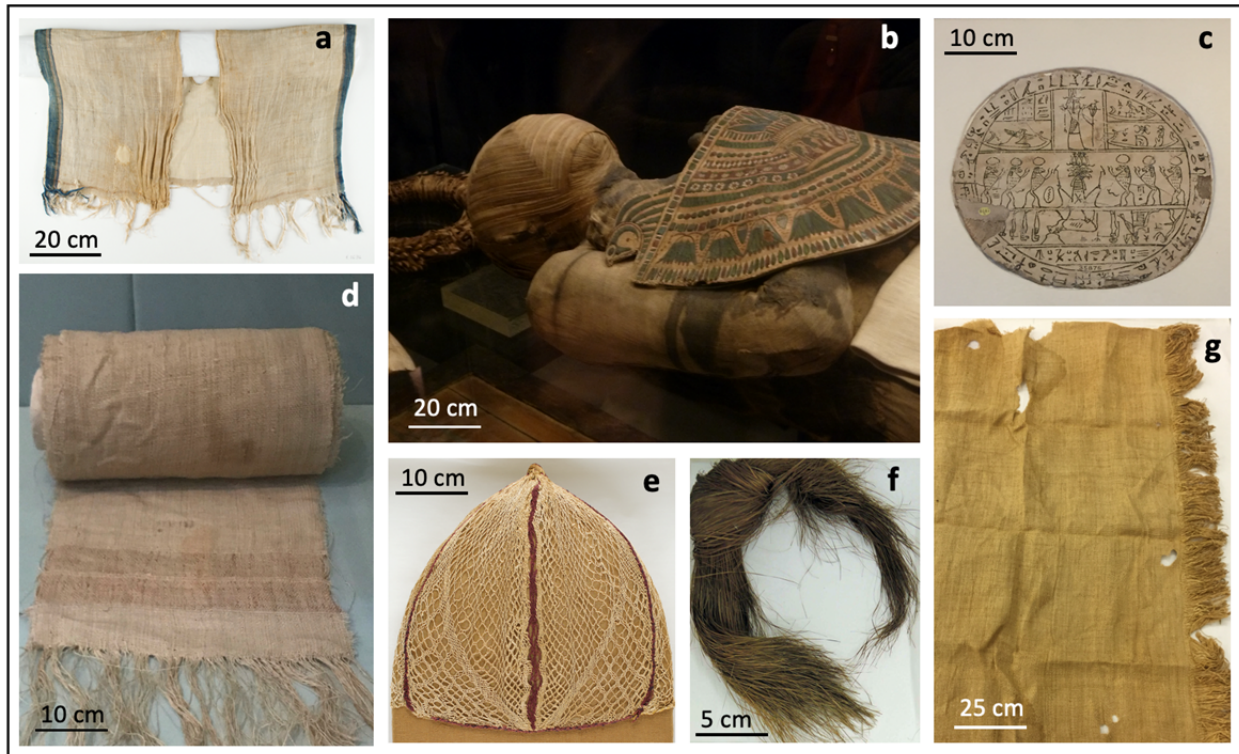


Fig. 1. Examples of the uses of flax in ancient Egypt. Child's vest with dyed blue edges, 800-720 or 700-540 BCE (a); Mummy of man with flax agglomerated and stuccoed fabric, 332-30 BCE (b); Flax hypocephalus, 305-30 BCE (c); Fragment of flax shroud, 1550-1295 BCE (d); Hairnet cap, AD 5th or 6th century (e); Unspun flax hank, 1420-1230 BCE (f) and Mortuary linen, 2140-1976 BCE (g). Objects c and d are exposed at the British Museum (London-UK); a, b, e, f and g are exposed (b) or in the store room (a, e, f and g) at the Louvre Museum (Paris-F). All images are from the authors' personal collection.

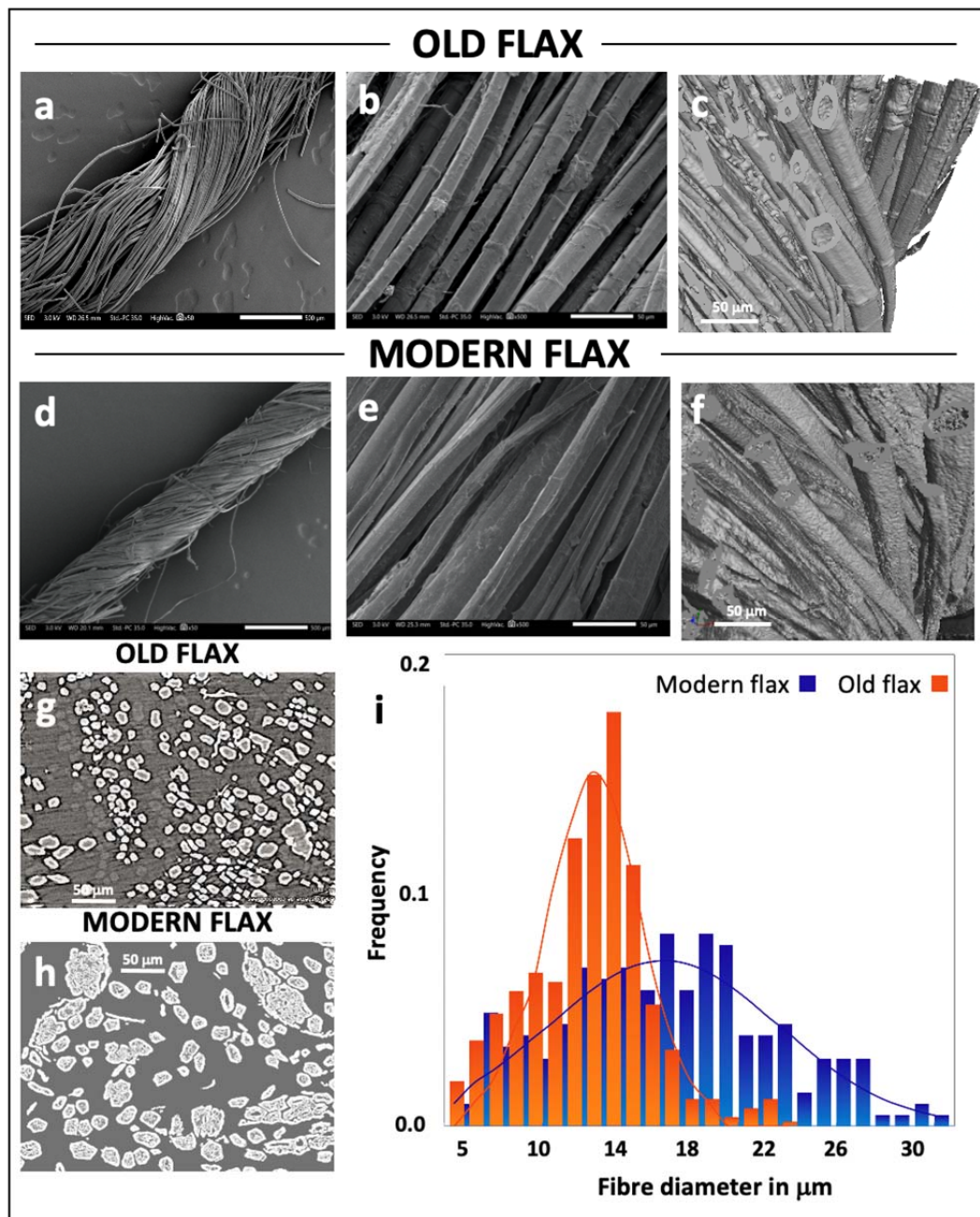


Fig. 2. Scanning electronic microscopy and nano-tomography images of modern and 4000-year-old flax. Overview of yarn (a, d) and fibres within the yarns (b, e); Tomographic overview of fibres highlighting the larger lumen size for old flax (c, f) and tomographic yarn cross-section showing the lower diameter of old flax fibres (g, h). Histograms (i) present the distribution of single fibre diameter for both old and modern flax.

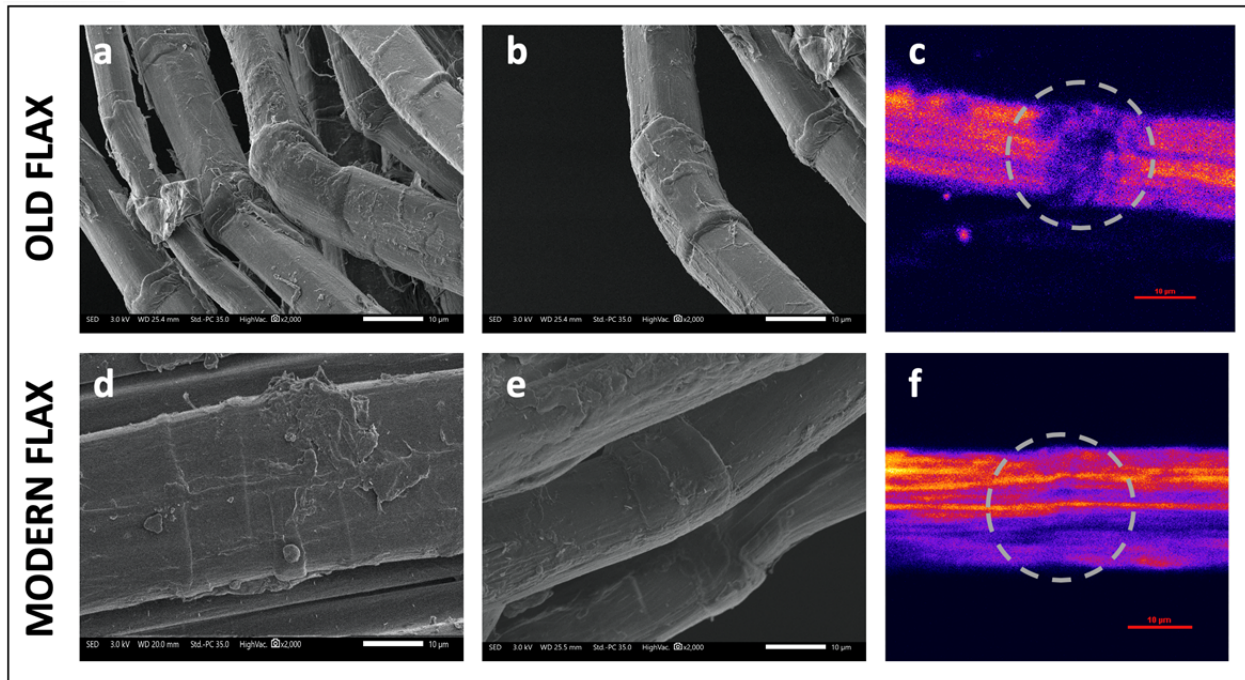


Fig. 3. Focus on kink-band (defect) regions in the fibres. Scanning electron microscopy images showing differences between kink-bands structure and intensity in old (a, b) and modern (d, e) flax. SHG microscopy observations highlighting the local disorganization of cellulose macrofibrils in the kink-band region for old flax (c) compared to modern flax (f). In Figures 3.c and 3.f, kink band region is circled by the dotted grey line.

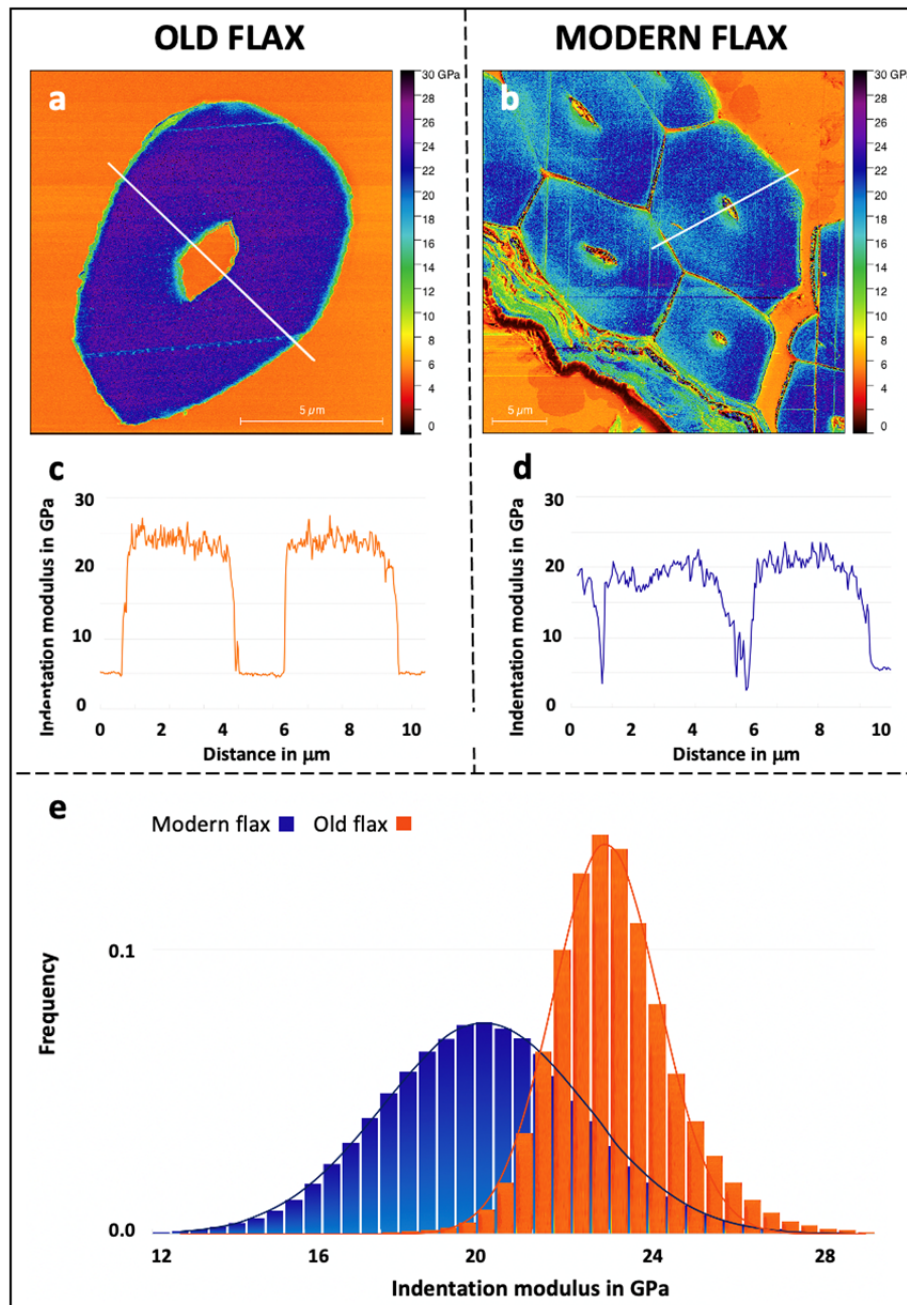


Fig. 4. AFM peak force measurements in old and modern flax fibres. One can notice larger lumen size on old flax fibre (a) and residue of cortical parenchyma on modern flax (b). Figure c and d show the profile of indentation modulus in old (c) and modern (d) flax according to the position on the white line (a and b). Distributions of indentation modulus are shown in (e); they are in good agreement with the preliminary nanoindentation tests performed (Supplementary Tab. 1).